Divergent impact of urban 2D/3D morphology on thermal environment along urban gradients

Andong Guo [a], Wenze Yue [a *], Jun Yang [b], Tingting He [a], Maoxin Zhang [a], Mengmeng Li [a, c]

[a] *Department of Land Management, Zhejiang University, Hangzhou 310058, China*

[b] *Jangho Architecture College, Northeastern University, Shenyang 110169, China*

[c] *Institute for Environmental Studies (IVM), VU University Amsterdam, Amsterdam 1081HV, The Netherlands*

*** Corresponding authors:**

Email: wzyue@zju.edu.cn (W. Yue)

This is the preprint version of an article published in *Urban Climate*:

Guo, A., Yue, W., Yang, J., He, T., Zhang, M., & Li, M. (2022). Divergent impact of urban 2D/3D morphology on thermal environment along urban gradients. *Urban Climate*. 45, 101278. https://doi.org/10.1016/j.uclim.2022.101278

Abstract: Optimizing urban morphology is an effective way to alleviate the thermal environment, and it has always been the focus of urban planning. Although previous scholars have explored the impact of urban 2D/3D morphology on Land Surface Temperature (LST), they have rarely revealed differences along urban gradients, and ignored the nonlinear relationship between urban morphology and LST. In this study, we use multi-source data such as night-time lights, Landsat 8, land cover, and buildings, and employ dynamic threshold, single-window algorithm, and boosted regression trees methods to reveal the gradient and marginal effects of urban 2D/3D morphology on LST. Results showed that the proportion of built-up land (PCL), digital elevation model (DEM) and normalized difference built-up index (NDBI) have important contribution to LST. Moreover, relative influence of PCL, NDBI and building density (BD) on LST varies significantly along urban gradients, which are +25.87%, +14.85% and -10.88%, respectively. Interestingly, we found that as the value of each variable increased, its relationship to LST changed. For example, when PCL < ~48%, it is negatively correlated with LST, so lowering PCL can alleviate thermal environment. Our findings inform the sound practice of urban planning by accounting for marginal effects of urban morphology on thermal environment.

Keywords: Land surface temperature; Built-up area; Urban morphology; Gradient effect; Boosted regression trees

1 Introduction

Since the Chinese policy of *Reform and Opening-up* implemented in 1978, rapid urbanization process in China has altered urban form and terrestrial surface (Seto et al.; Yue et al., 2019a). The continuous growth of impervious surface, building density and floor area ratio has led to the increasingly prominent high temperature extremes, which enormously affect the ecological environment and public health (Cai et al., 2018; He et al., 2021; Luo et al., 2021). Previous studies have shown that urban residents living under persistent high temperature conditions are more prone to cardiovascular and respiratory diseases (Patz et al., 2005). Therefore, in the context of global warming and urban expansion, optimization of the urban morphology to improve the thermal environment has received continuous attention from scholars and planning authority.

Urban Heat Island (UHI) mainly refers to the phenomenon of higher temperature in urban areas than that in their peripheries, mostly due to the modifications of urban underlying surface through human activities (Oke, 1973; Weng, 2009). Luke Howard (2012) divided the scope of UHI into three parts, i.e., the canopy layer, boundary layer, and land surface temperature (LST) heat island, in his book *The Climate of London*. Among them, LST is closely related to people's lives and has received extensive attention from scholars (Li et al., 2013; Yao et al., 2017; Liu et al., 2020). To mitigate urban heat, previous studies have extensively explored the impact of urban form on LST (Yao et al., 2019; Guo et al., 2020a). For example, Estoque et al. (2017) investigated the impact of impervious surface and green spaces on LST in Southeast Asian megacities and showed that the LST of impervious surface was 3°C higher than that of green spaces. Peng et al. (2020) investigated the cooling effect of water landscape and showed that the cooling intensity of water has significant spatial heterogeneity, with an average cooling of 1.1 °C. Thus, urban form is an important factor affecting LST, and optimizing its pattern is beneficial to alleviate urban high temperature.

However, previous studies on influencing factors of LST have mainly focused on 2D urban forms, such as blue-green spaces (i.e. water bodies and green spaces) and impervious surface area (Qiao et al., 2013; Wu et al., 2019; Yu et al., 2020a). Due to the limitation of building data, scholars rarely explore the influence of 3D morphology on LST (Yang et al., 2018; Li et al., 2020). Previous studies have shown that urban 3D buildings not only increase the absorption of solar radiation, but also reduce the natural ventilation of the city, resulting in a high concentration of urban heat (Yang et al., 2019; Yu et al.; Guan et al., 2021). For example, Berger et al. (2017) investigated the influence of 2D/3D urban site characteristics on LST in Berlin and Cologne using the Pearson correlation method and showed that 3D metrics had lower impact than 2D metrics (e.g., impervious surface area and vegetation fraction). Huang and Wang (2019) used Pearson correlation analysis to study the effect of 3D morphology in urban functional areas on LST, which suggests that LST is related to the composition and configuration of buildings. Thus, to thoroughly investigate the impact of urban form on LST, urban vertical landscape should not be ignored.

Although scholars have done a lot of work to explore the influence of 2D/3D morphology on LST, they mostly focus on the correlation of a single variable, ignoring the marginal effect of each parameter

on LST. The marginal effect of a variable refers to keeping other variables constant, as the independent variable increases, revealing the dynamic relationship between it and the dependent variable. Here, the marginal effect can reveal the non-linear relationship between urban form and LST, so as to optimize its pattern to alleviate the thermal environment to the greatest extent (Wang et al., 2021; Huang and Wang, 2022). In addition, human activities and urban morphology vary greatly along urban gradients, resulting in significant spatial heterogeneity of LSTs. Mastering the LST driving force within each gradient is more conducive to optimizing resources to alleviate the thermal environment. However, previous studies mostly explored the LST impact at a regional, city, block or grid scales (Liu and Weng, 2009; Yang et al., 2020), and lacked investigation of the main factors and dynamic changes affecting LST within each gradient. Therefore, exploring the gradient and marginal effects of urban form on LST is not only conducive to formulating corresponding strategies for each gradient, but also conducive to maximizing the optimization of urban morphology to alleviate the thermal environment.

Thus, in order to comprehensively understand the divergent impacts of urban morphology on LST, we combine 2D/3D morphology to reveal its gradient and marginal effects on thermal environment, to provide empirical support for cities in terms of adaption and mitigation to climate change. This paper consists of the following three parts: (1) explore the gradient effect of LST, (2) analyze the relative influence of urban morphology on LST along urban gradients via the boosted regression trees, and (3) reveal the marginal effect of urban morphology variables on LST. The in-depth analysis of the impact of urban spatial form on the LST provides empirical help determine how to effectively alleviate UHIs in the practices of urban planning.

2 Materials and methods

2.1 Study area

Beijing is not only the capital and primary megacity of China but also a political, cultural, and international exchange center (Fig. 1). The city is located between 115.7°E–117.4°E and 39.4°N–41.6°N in the northern part of the North China Plain, adjacent to Tianjin and Bohai Bay in the east and surrounded by Hebei Province on the other three sides. It is hot and rainy in the summer but cold and dry in the winter. As of 2020, the city contained 16 districts, including Dongcheng, Xicheng, Chaoyang, and Haidian, accommodating 21.9 million people. In recent years, to meet the living needs of the highly

dense urban population, the city's spatial form has undergone great changes, and the UHI has become increasingly prominent (Liu et al., 2020). Therefore, this study used Beijing as an example to explore the impact of urban morphology on the thermal environment to provide empirical support for spatial planning.

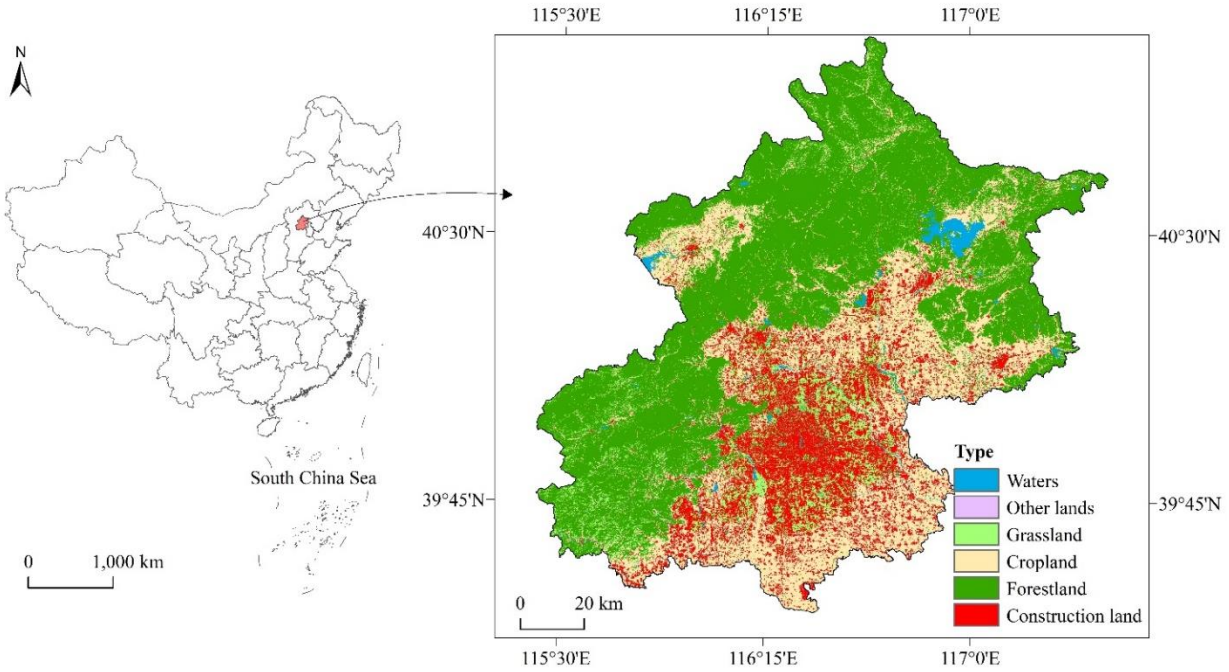

Fig. 1. Geographical location of the study area

2.2 Data

In this study, we used spatial data from multiple sources. Suomi National Polar-orbiting Partnership Visible Infrared Imaging Radiometer Suite (NPP-VIIRS) data, which represents the intensity of nighttime light (NTL), was firstly used to extract urban built-up areas (see Section 2.3.1), identify urban centroid, and establish urban gradients. Table 1 gives an overview of datasets used in this study. Specifically, Landsat-8, meteorological and MODIS data were used to retrieve and validate LST. Land use, building footprints and height, population, and DEM data were used to extract urban 2D/3D morphological variables, representing independent variables that influence LST.

Table 1 Data description

Data	Description	Source
Landsat 8	Beijing (path: 123, row: 32), Date: July 10, 2017	Geospatial data cloud(http://www.gscloud.cn/search)
DEM	30 m	

Population	2017, 100 m	https://www.worldpop.org/
NTL	2017, NPP-VIIRS (500 m)	https://eogdata.mines.edu/products/vnl/
Land use/cover	2017, 10 m	http://data.ess.tsinghua.edu.cn/
Building	2017	Baidu API
Meteorological data	Date: July 10, 2017	National Weather Data Center (http://data.cma.cn/)
MOD11A2	2017, 1 km	https://ladsweb.modaps.eosdis.nasa.gov/search/

2.3 Methods

As depicted in Fig. 2, our analytical framework consists of three components: (1) retrieve LST and explore its gradient changes, (2) extract urban 2D/3D morphological parameters from multi-source data, and (3) explore the impact of urban morphology on LST via the BRT method.

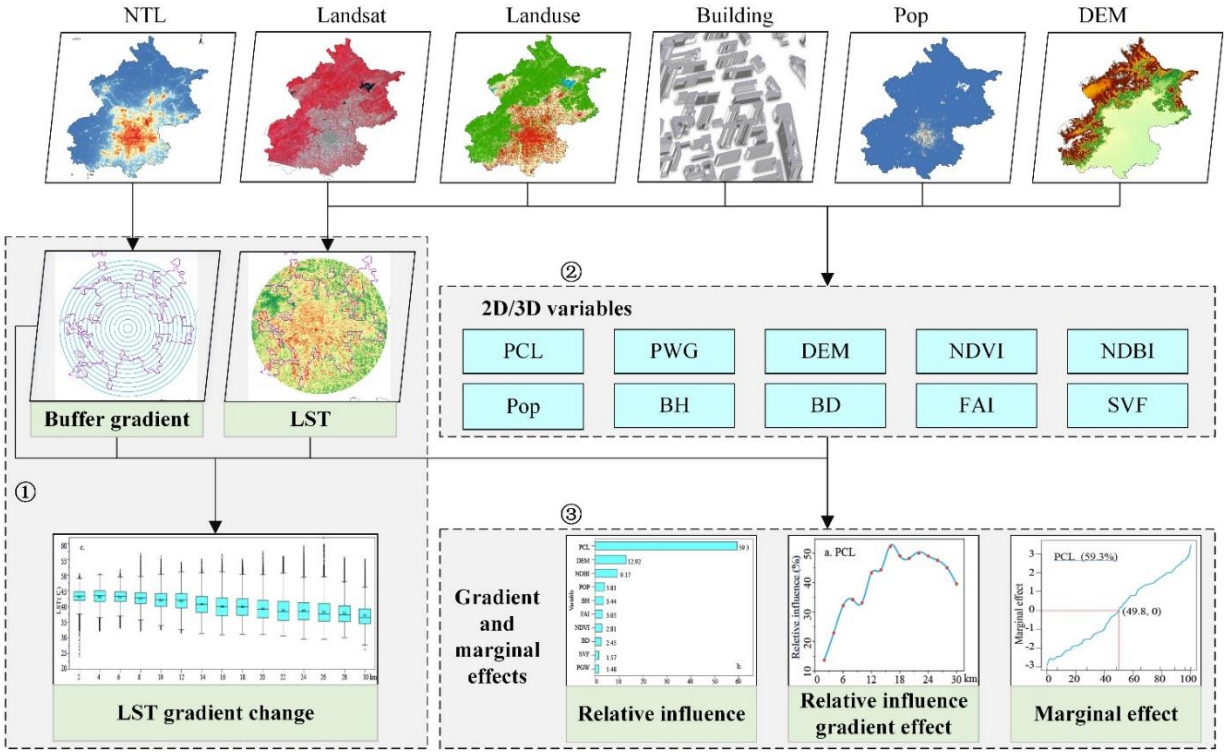

Fig. 2. Specific workflow of this study

2.3.1 Extraction of built-up areas

Compared to conventional optical remote sensing data, NTL can better represent human activities and thus has been widely used in estimating population density and energy consumption as well as identifying construction land and built-up areas (Liu et al., 2012; Bennett and Smith, 2017). A wide range of method have been used to extract built-up areas from NTL imageries, including dynamic optimal threshold, mutation detection, image segmentation, and fusion with other high-resolution

images (Tong et al., 2018; Zhou et al., 2018), among many others. In this paper, we identify built-up areas based on the characteristics of NPP-VIIRS radiation values in built-up areas, urban-rural transition areas, and rural areas, highlighting the "suburban" lighting differences. First, we logarithmically process the NPP-VIIRS data to compress the range of light radiation in the built-up area and stabilize the change of light radiation (Yu et al., 2018). Second, combined with dynamic threshold method and statistical data, the built-up area and centroid are determined. Finally, we establish a 2-km buffer gradient based on the city centroid, which builds the foundation for the subsequent exploration of the impact of urban morphology on LST.

2.3.2 Land surface temperature retrieval

LST retrieval methods from thermal infrared remote sensing images mainly include the radiative transfer method, split-window algorithm, and single-channel algorithm (J. et al., 2014; Kotharkar et al., 2018). Qin et al.(2001) used the single-window algorithm to retrieve LST on the basis of the characteristics of TM data with only one thermal infrared band. In the present study, the digital number (*DN*) value was converted into the corresponding radiation intensity value (L_λ) according to Planck's formula, and the corresponding radiation brightness value (T_a) was further obtained. The specific formulas are as follows:

$$L_\lambda = Gain \times DN + Offset \quad (1)$$

$$T_a = \frac{K_2}{\ln(1+\frac{K_1}{L_\lambda})} \quad (2)$$

where L_λ is the radiation intensity value; T_a is the radiation brightness value; and Gain and Offset represent the gain and offset parameters, respectively, which can be found in the header file of the Landsat imaginary. Moreover, *DN* is the gray value of the thermal infrared band; K_1 = 774.89 mW/(cm^2·sr·μm), and K_2 = 1,321.08 K.

The LST calculation formula is as follows:

$$T_s = \frac{\left(a(1-C-D)+T_a(b(1-C-D)+C+D\right)-DT_b}{C} - 273.15 \quad (3)$$

$$C = \varepsilon\tau \quad (4)$$

$$D = (1-\tau)[1+(1-\varepsilon)\tau] \quad (5)$$

where T_s represents LST, and T_a is the radiation brightness value (K), T_b is the average atmospheric temperature (K), C and D are intermediate variables, and a and b are the fitting coefficients based on the thermal radiation intensity (when the temperature was between 0 °C and 70 °C, $a = -67.355351$, and $b = 0.458606$). Moreover, ε and τ are the surface emissivity and atmospheric transmittance in the thermal infrared band, respectively. Here, τ was calculated according to the atmospheric parameters recommended by NASA (http://atmcorr.gsfc.uasa.gov/).

In addition, we verify the accuracy of LST values by combining meteorological and MODIS data. MODIS data has been widely recognized by scholars in exploring the thermal environment (Wan, 2008; Peng et al.; Yao et al., 2021). However, due to its low spatial resolution (1 km), it fails to spatially match the LST retrieval results. Therefore, we divide into a 3 km × 3 km grid and count its LST mean. Finally, we find that the LST retrieval results have high accuracy and can reflect its spatial characteristics.

2.3.3 Urban 2D/3D morphology parameters

The transformation of urban form has a far-reaching impact on UHI. Hence, it is of great significance to explore the influence of the urban 2D/3D morphology on LST to steer planning interventions aiming to mitigate climate change (Yue et al., 2019b; Yang et al., 2021a). In this paper, 2D/3D morphological parameters mainly refer to land use/cover type, population, and building morphology. Consistent with existing studies, we selected 10 parameters, including the PCL, the proportion of woodland and grass (PWG), DEM, and BD (Table 2) (Peng et al., 2018; Zhou et al., 2019; Guo et al., 2020b), and used the BRT method to explore the impact of each urban morphology on the LST.

Table 2 Description of urban 2D/3D factors

Type	Variables	Description
2D	Proportion of construction land (PCL)	Represents the proportion of the construction land area in each grid (%)
	Proportion of woodland and grass (PWG)	Represents the proportion of woodland and grass area in each grid (%)
	Digital elevation model (DEM)	Represents the mean value of the DEM in each grid
	Normalized difference vegetation index (NDVI)	Represents the mean value of the NDVI in each grid
	Normalized difference built-up index (NDBI)	Represents the mean value of the NDBI in each grid
	Population (Pop)	Represents the population in each grid
3D	Building height (BH)	Represents the average building height in each grid
	Building density (BD)	Represents the building density in the grid
	Frontal area index (FAI)	Represents the frontal area index in the grid
	Sky view factor (SVF)	Represents the sky view factor in the grid

2.3.4 Boosted regression trees

Boosted regression trees (BRT) is a machine-learning statistical method that primarily improves the performance of individual models by synthesizing multiple models and implementing final predictions (Elith et al., 2008). It comprises a decision-tree architecture and a boosting algorithm. It outperforms other models given that the interaction between independent variables does not need to be considered, and the contribution of independent variables to dependent variables and the response curve can be obtained (Carslaw and Taylor, 2009). Decision trees are popular primarily because they represent information in an intuitive and easy-to-visualize way. The predictive variables can be of any type (numeric, binary, categorical, etc.). In addition, the model results are not affected by monotonic transformation of predictors or measurement scales, and less uncorrelated predictors are selected, thus simplifying the preparation of candidate predictors. Boosting is a method used for improving prediction accuracy, with the advantage of being a forward, phased, and continuous process (Hu et al., 2020; Li and Hu, 2022).

Overall, the BRT method has superior predictive performance and reliability to identify the interactions among multiple variables. It has been widely used in many fields, such as urban expansion, farmland abandonment, and thermal environment research (Müller et al., 2013; Sun et al., 2019; Yuan et al., 2021a). In this study, it was used to reveal the relative and marginal effects of urban morphology on LST. The algorithm was mainly implemented through the third-party packages "*dismo*" and "*gbm*"

in the R software. The specific parameters were as follows: family = “laplace,” tree.complexity = 5, learning.rate = 0.01, and bag.fraction = 0.5.

3 Results

3.1 Gradient effect of the LST

Fig. 3a shows that built-up area in Beijing was mainly in the central area of the city, exhibiting a polycentric mode in space. Here, we extract centroids based on built-up areas and establish buffer gradients with a 2-km interval to explore the variation of LST (Fig. 3b). Then, we analyze the spatial pattern of LST within each buffer zone and serve as an important basis for the subsequent exploration of their driving forces. Fig. 3b, c shows that the high value of LST is mainly distributed around the urban centroid, and shows a certain gradually decreasing trend. With increasing distance from the urban centroid, LST gradually decreases spatially, from 43.11°C to 37.16°C, with a total decrease of 5.95°C.

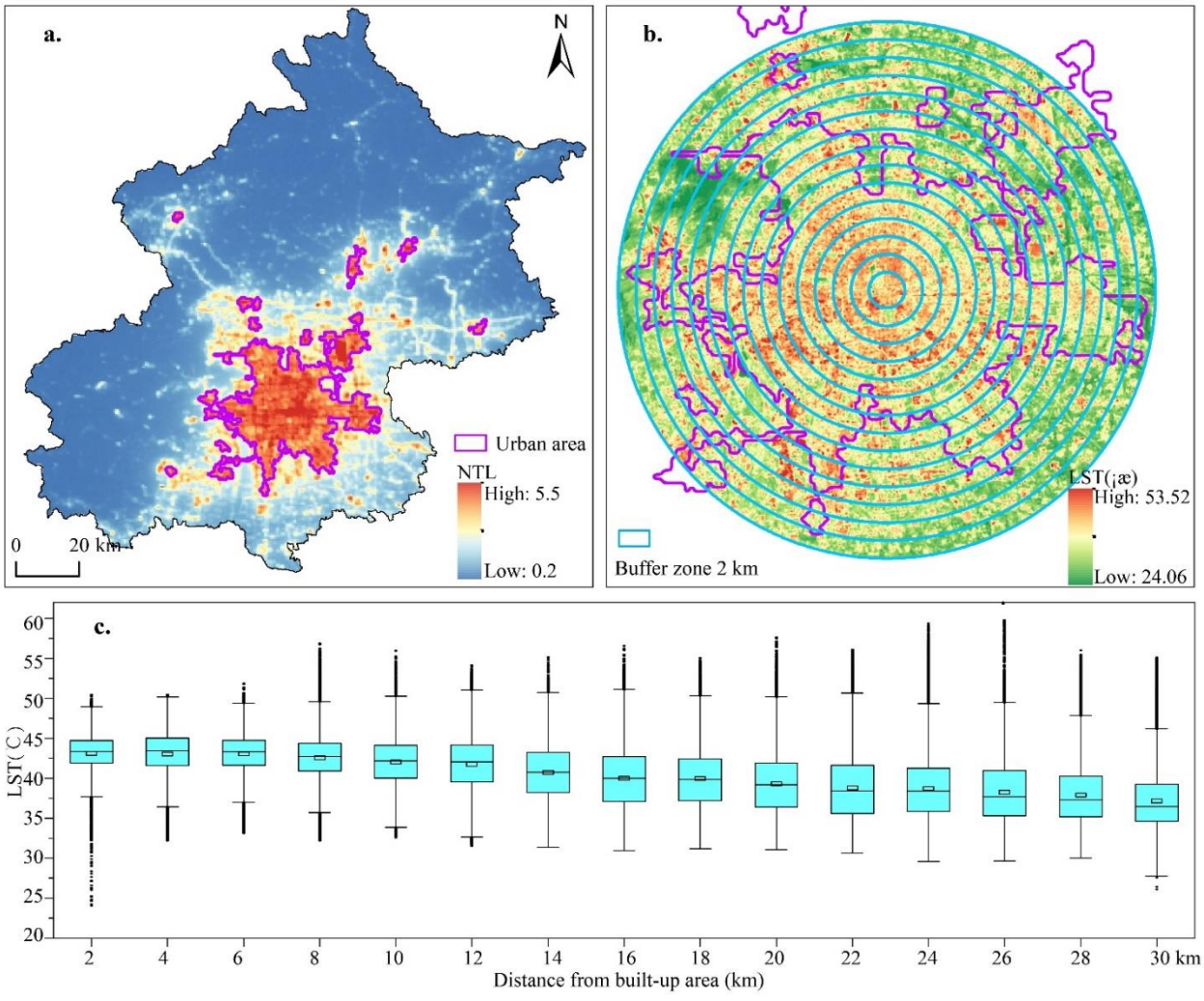

Fig. 3. Spatial characteristics of the built-up area and LST (a. represents the nighttime light image and built-up area, b. represents the 2 km buffer gradient of LST, and c. represents LST within each gradient range)

3.2 Relative influence of urban morphology on LST

3.2.1 Impact of urban morphology on LST along urban gradients

Fig. 4 shows that the impact of urban morphology on LST varies greatly along urban gradients. In general, PCL is the most important variable affecting LST in each buffer zone, with a relative impact of 52.67% when it is 16 km away from the city center. BH and BD are important 3D factors affecting LST, and they have the highest impact at 6 km from the city center, with 11.78% and 11.09%, respectively. In addition, we found that compared with 2D metrics, 3D has substantial impacts on LST compared to 2D metrics (DIS < 12km), except PCL and DEM. The main reason is that the distance from the city center increases and the number of 3D buildings in the city gradually decreases.

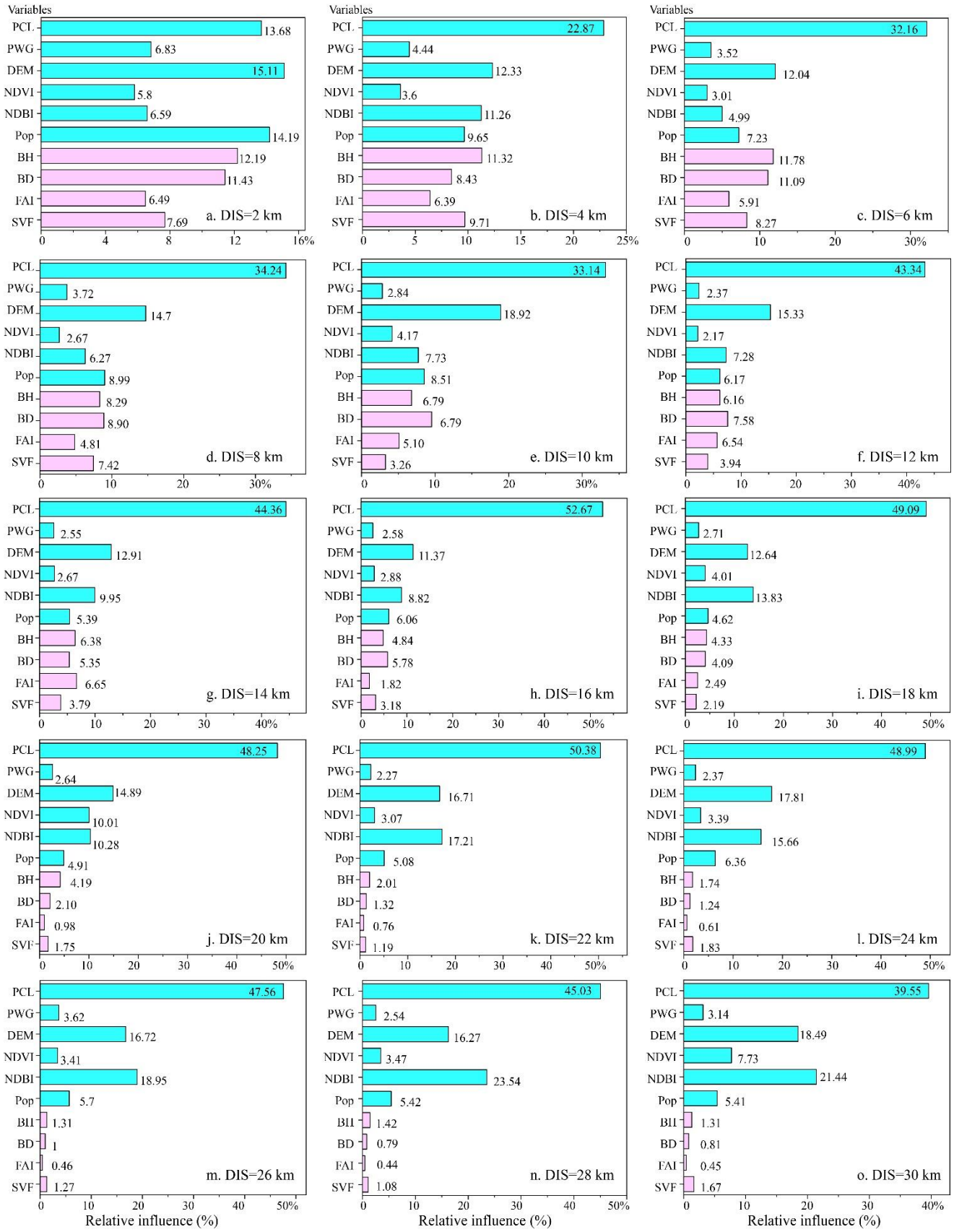

Fig. 4. Relative influence of each variables on LST along urban gradients. The cyan and orchid bars denote 2D and 3D variables, respectively. DIS is the distance from the city center.

In addition, we grouped them into 4 processes with distances of 2, 6, and 16 km from the city center, respectively, according to the differences in LST impact factors within each buffer. Specifically, in the case that DIS equals 2 km, the difference of 2D/3D factors on LST is minimal, given that the urban land is intensively used in a homogeneous manner. When DIS<6 km, variables do not change significantly except PCL. Moreover, BD, BH and SVF have higher influence than other 2D factors. When DIS<16 km, PCL and DEM were important factors, with mean values of 41.55% and 14.65%, respectively. However, the effect of 3D factors on LST gradually decreased. PCL, DEM and NDBI were the main variables affecting LST (DIS<30), with mean effects of 46.98%, 16.22% and 24.18%, respectively. In summary, 6 km and 16 km from the city center of Beijing are the best distances to explore the effects of 3D and 2D on LST, respectively.

3.2.2 Gradient effect of urban morphology on LST

Fig. 5 shows that the effects of PCL and NDBI on LST are significantly different. Specifically, the impact of PCL increased from 13.68% (DIS=2 km) to 52.67% (DIS=16 km), a total increase of 38.99%. The influence of NDBI increased from 6.59% (DIS=2 km) to 21.44% (DIS=28 km), a total increase of 14.85%. We can see that PCL and NDBI have the greatest impact on LST at 16 km and 28 km from the city center, respectively. However, the effects of FAI, SVF, BH and BD on LST gradually decreased with increasing distance, decreasing by 6.04%, 6.02%, 10.88% and 10.62%, respectively. This change is due to the gradual decrease in population density and buildings with increasing distance from the city center.

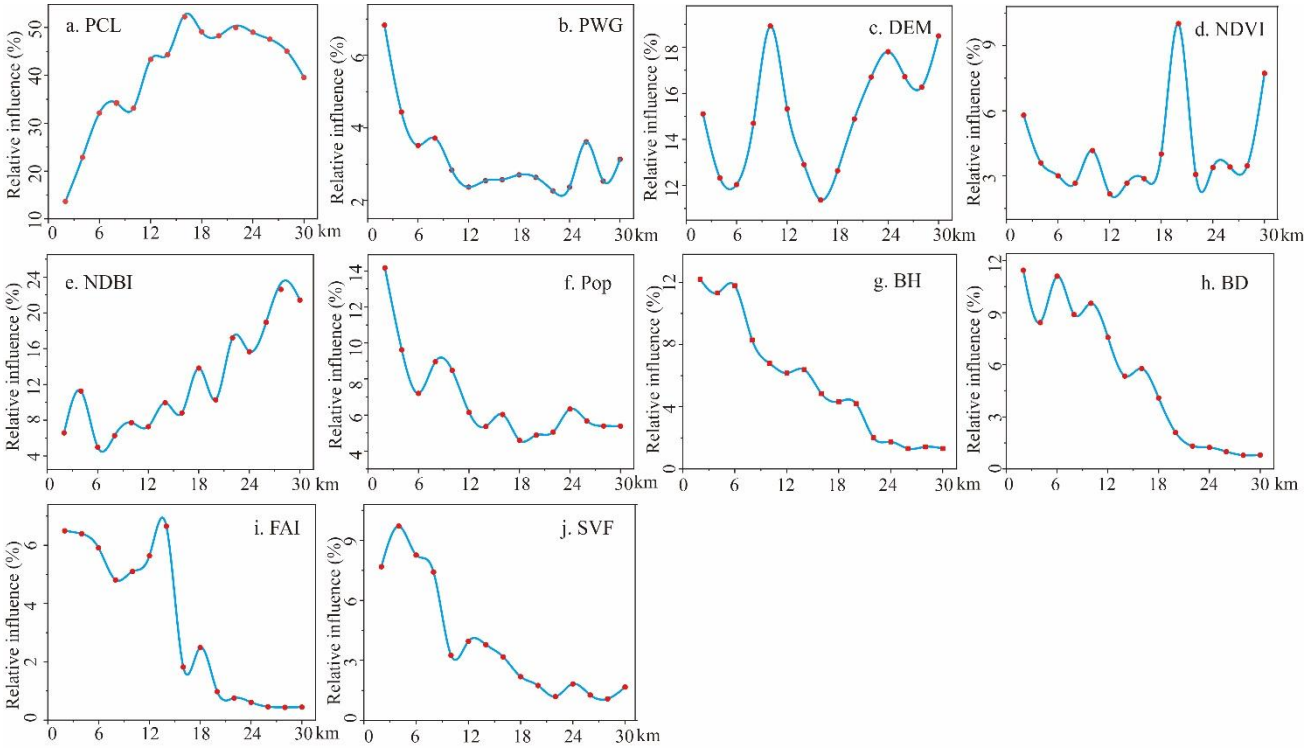

Fig. 5. Gradient effect of each variable on LST

3.3 Marginal effect of urban morphology on LST

The horizontal and vertical axes in Fig. 6 represent the range of each factor and its influence on LST, respectively. Specifically, vertical axis values <0, 0, and >0 indicate that each variable is negative, uncorrelated, and positive correlations with LST, respectively. Also, the larger the absolute value, the higher its influence. We select the main variables that affect LST in each buffer gradient, such as PCL, DEM, NDBI, BH, etc., to reveal the marginal effect of each factor on LST.

According to the marginal effect of LST, it can be classified into four types: "negative-positive", "negative-positive-stable positive", "positive-negative-stable negative" and "positive-negative" (Fig. 6). Specifically, as the value of each factor increases, its correlation with LST changes. Fig. 6 shows that PCL and DEM are important factors affecting LST. Among them, PCL=47.79% is the inflection point of the "negative-positive" relationship of LST. As PCL increased, its correlation with LST gradually increased. The relationship between DEM and LST is complex. When the DEM is approximately between 40 m and 200 m, it is positively correlated with LST, because of the frequent human social activities in this area. The other areas of the DEM are suburbs, which are farmland and woodland, which are negatively correlated with LST. In addition, when NDBI and BD are about -0.1 and 31.75,

respectively, it is the inflection point of the positive and negative relationship with LST. Hence, urban planning should avoid blind expansion, resulting in the exacerbation of urban heat islands.

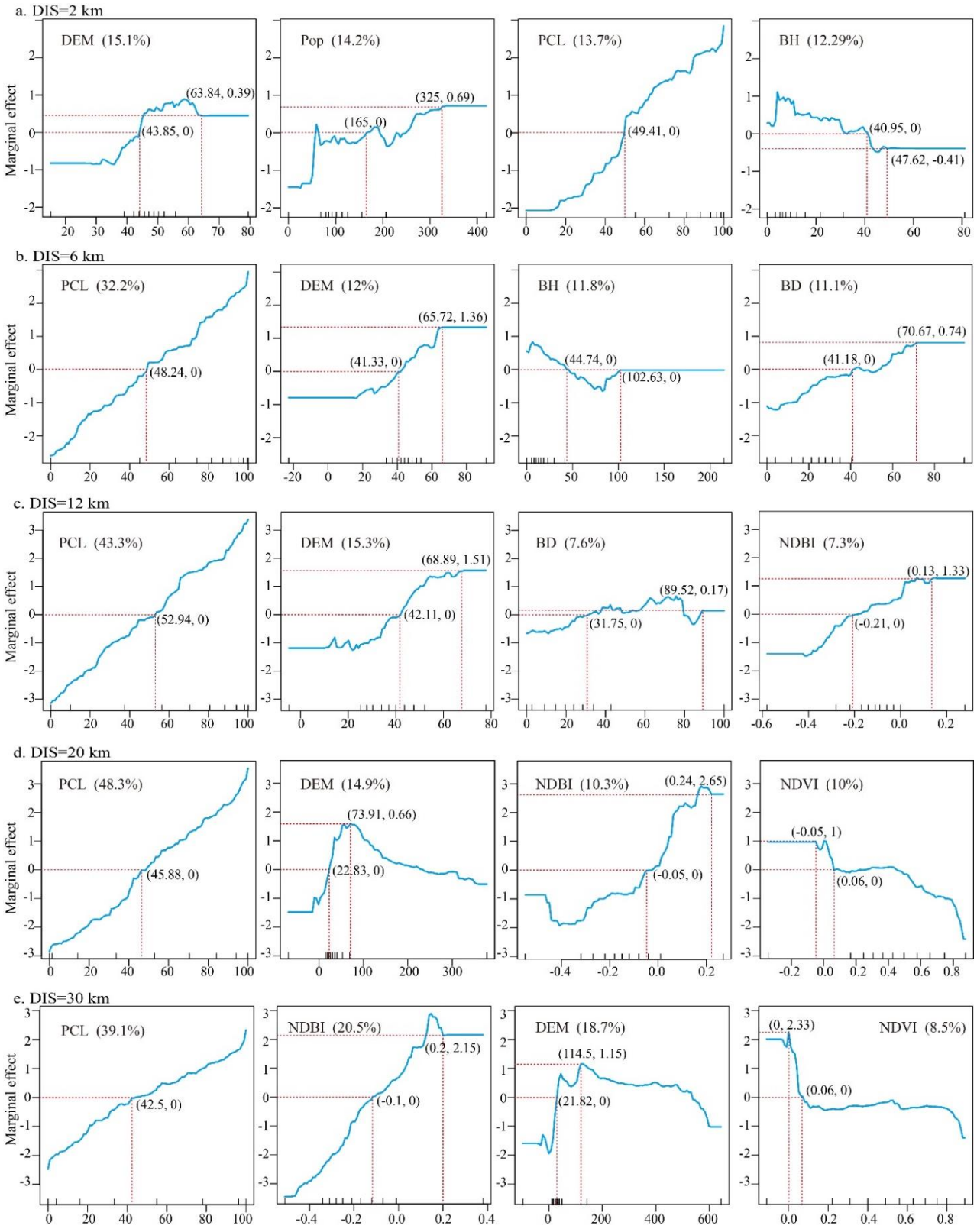

Fig. 6. Marginal effect of each variable on LST

However, BH and NDVI had opposite characteristics to LST correlation. That is, as the value increases, it is negatively correlated with LST. For example, when BH is greater than about 40 m, it is negatively correlated with LST. The main reason is that the shading area of buildings increases with the increase of BH. It can be seen that the BH height not only has a warming effect, but also a cooling effect. NDVI is mostly used to reflect vegetation coverage. Higher values represent lush vegetation and good shading. When NDVI>0.06, it was negatively correlated with LST. Thus, in areas with a wide distribution of buildings, the green area should be increased to relieve high temperature and improve comfort.

4 Discussion

4.1 Difference of 2D/3D morphology on LST

The impact of urban morphology on thermal environment has been extensively studied (Stewart et al., 2014; Lu et al., 2021). However, due to the limitation of building height data, there are only a few studies exploring the influence of 3D morphology on LST (Zhang et al., 2019). Moreover, scholars have different views on the impact of 2D/3D morphology on LST (Liu et al., 2021; Yuan et al., 2021b) . In this study, we found that with the increasing distance from city center, PCL was continuously the key factor affecting LST, with a peak contribution of 52.67% (Fig. 4). Second, the effects of NDBI and NDVI on LST are quite different. Fig. 7 shows that the Pearson correlations of NDBI and NDVI and LST are 0.75 and -0.78, respectively, indicating that they have a high correlation with LST. However, we combined many factors and found that the effect of the two on LST was less than 10%. This result is different from previous studies (Hu et al., 2020). The reason may be that PCL is higher resolution land cover data (10 m), while NDBI and NDVI have lower resolution (30 m), resulting in different results. In addition, DEM is also an important factor affecting LST, about 13%. The reason is that with the increase of altitude, different slope aspects and slopes affect the absorption of solar heat energy by the surface, which in turn leads to different LSTs. It can be seen that the DEM is an important factor affecting LST.

Interestingly, we found that the impacts of BH and BD on LST around the city center are in equilibrium with 2D factors (Fig. 4). It suggests that 3D morphological parameters cannot be ignored when exploring the thermal environment in dense cities. Urban planning authorities should control

building height and density, reduce their heat absorption, and plan ventilation corridors to mitigate urban heat islands.

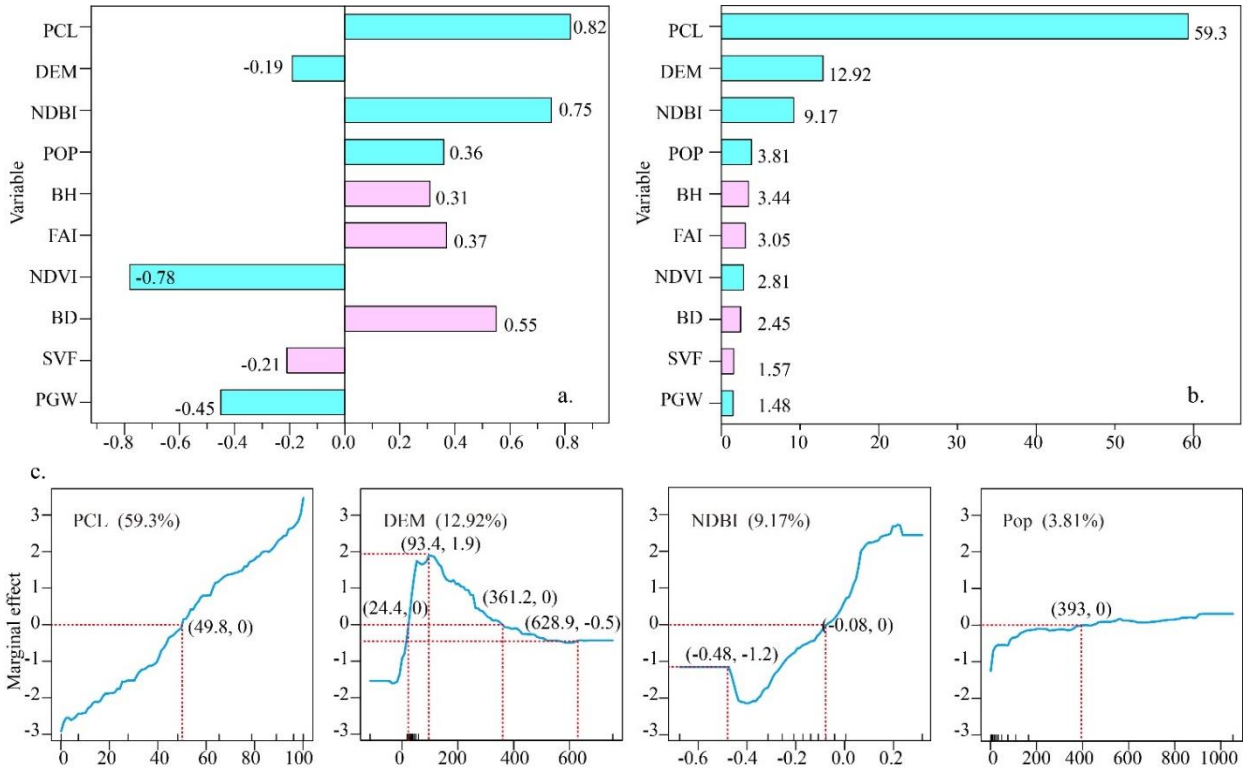

Fig. 7. Impact of urban morphology variables on LST (a. represents the Pearson correlation, b. represents the relative impact of the BRT, and c. represents the marginal effect of the BRT. The cyan and orchid bars denote 2D and 3D variables, respectively.

4.2 Marginal effect of 2D/3D morphology on LST

Previous studies on the effect of 2D/3D morphology on LST used the Pearson correlation (Huang and Wang, 2019; Ezimand et al., 2021; Yang et al., 2021b) (Fig. 7a). However, this method can only identify positive or negative correlations and cannot diagnose their dynamic changes (Li et al., 2021). This study addresses this issue by adopting the BRT method, revealing the marginal effect of each factor on the LST, which better informs the practice of urban planning (Fig. 7c). For example, the Pearson correlations of BH and BD and LST are 0.31 and 0.55, respectively, that is, there is a significant positive correlation. However, Fig. 6 shows that the correlation with LST becomes negative when BH is greater than 40 m. This result is consistent with previous studies, which can be attributed to two reasons (Hu et al., 2020; Li et al., 2021). First, the height difference of the building is large, which makes it easier to form air vents and intensifies the accumulation of wind on the surface. Second, high-rise buildings

tend to cast more shadows, which have a cooling effect on the area (Park et al., 2021). In addition, when BD>35, there is a positive correlation with LST, increasing regional LST. Therefore, the marginal effect can clearly reveal the influencing factors of LST.

Also, we found a significant positive correlation with LST when PCL was greater than 49%. Therefore, urban development in highly urbanized area is supposed to strictly constrain new construction land from the view of urban thermal environment. Prior studies have predominantly explored the impact of land cover, buildings and trees on LST, while the impact of DEM on LST is less discussed (Zeng et al., 2022). We find a substantial variation in the relationship between DEM and LST. In particular, DEM (<24.4m and >361.2m) was negatively correlated with LST (Fig. 7c). A closer observation suggests that these regions are dominated by vegetation, which cool the air through evapotranspiration (Maimaitiyiming et al., 2014). Other areas, however, are concentrated by human activities, exacerbating the urban heat island effect due to anthropogenic heat and carbon emissions from vehicle exhaust.

4.3 Implications for urban planning and management

Studies have shown that urban morphology has significant impacts on LST, especially PCL and DEM. When PCL was greater than 49%, it was highly positively correlated with LST. Thus, cities are supposed to control the extent and magnitude of construction, optimize the spatial pattern of land use, and cool the city by expanding the area of open green space. Furthermore, BH and BD are important 3D morphological factors affecting LST. When BH and BD have larger and smaller values, respectively, the LST decreases. It can be seen that maintaining a reasonable building height difference and building density can control the air flow of the building, which in turn has a cooling effect for the area. In addition, compared with previous studies, NDVI has less than 10% effect on LST. Our speculation is that the area of green space in Beijing is much lower than that of the impervious layer, leading to a large amount of heat absorbed by the surface and aggravates the UHI. Hence, planning urban ventilation corridors according to buildings, roads, water bodies and green spaces could alleviate urban high temperature.

4.4 Limitations and future works

This study explored the divergent impact of urban 2D/3D morphology on thermal environment along urban gradients. However, there are some limitations. First, this study does not consider the

landscape characteristics, such as patch density, aggregation degree or fragmentation and other factors. Second, due to the absence of vegetation height data, we ignored the mitigation effect of tree canopy and height on thermal environment. Finally, we only carried out the study with a 100m grid, and did not consider the effect of different scales on the results. In the future, we will combine multi-source datasets (including LiDAR) to extract vegetation heights, so as to improve the lack of LST influencing factors in urban form. In addition, since ventilation corridors are often constructed based on the three-dimensional form of the city, we will also quantify the impact of ventilation corridors on the thermal environment to provide guidance for urban planning.

5 Conclusions

This study investigated the impact of urban 2D/3D morphology on LST along the urban gradients of Beijing, which informs urban planning practices by accounting for the influence of various factors on LST. Specifically, we found that: (1) The influence factors of LST vary substantially along urban gradients. Within the city center (i.e., DIS=2 km), effect of each variable on LST is not very different. PCL, DEM and NDBI were the important factors affecting LST, with the highest values of 52.67% (DIS=16 km), 18.92% (DIS=10 km), and 23.54% (28 km), respectively. (2) Each factor has a significant gradient effect on the LST effect. The effects of PCL and NDBI on LST increased with increasing distance from the city center, while the effects of PWG, POP, FAI, SVF, BH, and BD gradually decreased. (3) In terms of marginal effects, the positive and negative relationship between the LST and the factors is dynamically changed. Among them, PCL and LST marginal effects are most obvious. That is, when the PCL is more than 48%, it is positively correlated with LST. We concluded that Beijing's urban planning authorities should reasonably control the scale of land development and increase green space in regions with a high BD to reduce the adverse impact of high temperature on residents' health.

6 Abbreviations

BRT	Boosted regression trees
BD	Building density
BH	Building height
DEM	Digital elevation model
DIS	Distance from the city center
DN	Digital number

FAI	Frontal area index
LST	Land Surface Temperature
NDBI	Normalized difference built-up index
NDVI	Normalized difference vegetation index
NPP-VIIRS	National Polar-orbiting Partnership Visible Infrared Imaging Radiometer Suite
NTL	Night-time light
PCL	Proportion of construction land
Pop	Population
PWG	Proportion of woodland and grass
SVF	Sky view factor
UHI	Urban Heat Island

Acknowledgments

This research study was supported by China Postdoctoral Science Foundation (2021M702789) and National Natural Science Foundation of China (grant no.41871169, 41771178). The authors would like to acknowledge all experts' contributions in the building of the model and the formulation of the strategies in this study.

References:

Bennett, M. M., & Smith, L. C., 2017. Advances in using multitemporal night-time lights satellite imagery to detect, estimate, and monitor socioeconomic dynamics. *Remote Sensing of Environment*. 192, 176-197. https://doi.org/10.1016/j.rse.2017.01.005

Berger, C., Rosentreter, J., Voltersen, M., Baumgart, C., Schmullius, C., & Hese, S., 2017. Spatio-temporal analysis of the relationship between 2D/3D urban site characteristics and land surface temperature. *Remote Sensing of Environment*. 193, 225-243. https://doi.org/10.1016/j.rse.2017.02.020

Cai, M., Ren, C., Xu, Y., Lau, K. K., & Wang, R., 2018. Investigating the relationship between local climate zone and land surface temperature using an improved WUDAPT methodology – A case study of Yangtze River Delta, China. *Urban Climate*. 24, 485-502. https://doi.org/10.1016/j.uclim.2017.05.010

Carslaw, D. C., & Taylor, P. J., 2009. Analysis of air pollution data at a mixed source location using boosted regression trees. *Atmospheric Environment*. 43(22), 3563-3570. https://doi.org/10.1016/j.atmosenv.2009.04.001

Elith, J., Leathwick, J. R., & Hastie, T., 2008. A working guide to boosted regression trees. *Journal of Animal Ecology*. 77(4), 802-813. https://doi.org/10.1111/j.1365-2656.2008.01390.x

Estoque, R. C., Murayama, Y., & Myint, S. W., 2017. Effects of landscape composition and pattern on land surface temperature: An urban heat island study in the megacities of Southeast Asia. *Science of The Total Environment*. 577, 349-359. https://doi.org/10.1016/j.scitotenv.2016.10.195

Ezimand, K., Azadbakht, M., & Aghighi, H., 2021. Analyzing the effects of 2D and 3D urban structures on LST changes using remotely sensed data. *Sustainable Cities and Society*. 74, 103216. https://doi.org/10.1016/j.scs.2021.103216

Guan, Q., Yao, Y., Ma, T., Hong, Y., Bie, Y., & Lyu, J., 2021. Under the dome: A 3D urban texture model and its relationship with urban land surface temperature. *Annals of the American Association of Geographers*, 1-21. https://doi.org/10.1080/24694452.2021.1972790

Guo, A., Yang, J., Sun, W., Xiao, X., Xia Cecilia, J., Jin, C., & Li, X., 2020b. Impact of urban morphology and landscape characteristics on spatiotemporal heterogeneity of land surface temperature. *Sustainable Cities and Society*. 63, 102443. https://doi.org/10.1016/j.scs.2020.102443

Guo, A., Yang, J., Xiao, X., Xia Cecilia, J., Jin, C., & Li, X., 2020a. Influences of urban spatial form on urban heat island effects at the community level in China. *Sustainable Cities and Society*. 53, 101972. https://doi.org/10.1016/j.scs.2019.101972

Hansen, J., Ruedy, R., Sato, M., & Lo, K., 2010. Global surface temperature change. *Reviews of Geophysics*. 48(4). https://doi.org/10.1029/2010RG000345

He, B., Wang, J., Liu, H., & Ulpiani, G., 2021. Localized synergies between heat waves and urban heat islands: Implications on human thermal comfort and urban heat management. *Environmental Research*. 193, 110584. https://doi.org/10.1016/j.envres.2020.110584

Howard, L. (2012). *The climate of London: Deduced from meteorological observations* (Vol. 1): Cambridge University Press.

Hu, Y., Dai, Z., & Guldmann, J., 2020. Modeling the impact of 2D/3D urban indicators on the urban heat island over different seasons: A boosted regression tree approach. *Journal of Environmental Management*. 266, 110424. https://doi.org/10.1016/j.jenvman.2020.110424

Huang, J., & Wang, Y., 2022. Cooling intensity of hybrid landscapes in a metropolitan area: Relative contribution and marginal effect. *Sustainable Cities and Society*. 79, 103725. https://doi.org/10.1016/j.scs.2022.103725

Huang, X., & Wang, Y., 2019. Investigating the effects of 3D urban morphology on the surface urban heat island effect in urban functional zones by using high-resolution remote sensing data: A case study of Wuhan, Central China. *ISPRS Journal of Photogrammetry and Remote Sensing*. 152, 119-131. https://doi.org/10.1016/j.isprsjprs.2019.04.010

J., C. J., J., A. S., D., S., C., M., & J., C., 2014. Land surface temperature retrieval methods from landsat-8 thermal infrared sensor data. *IEEE Geoscience and Remote Sensing Letters*. 11(10), 1840-1843. https://doi.org/10.1109/LGRS.2014.2312032

Kotharkar, R., Ramesh, A., & Bagade, A., 2018. Urban Heat Island studies in South Asia: A critical review. *Urban Climate*. 24, 1011-1026. https://doi.org/10.1016/j.uclim.2017.12.006

Li, H., Li, Y., Wang, T., Wang, Z., Gao, M., & Shen, H., 2021. Quantifying 3D building form effects on urban land surface temperature and modeling seasonal correlation patterns. *Building and Environment*. 204, 108132. https://doi.org/10.1016/j.buildenv.2021.108132

Li, M., Koks, E., Taubenböck, H., & van Vliet, J., 2020. Continental-scale mapping and analysis of 3D building structure. *Remote Sensing of Environment*. 245, 111859. https://doi.org/10.1016/j.rse.2020.111859

Li, Z., Tang, B., Wu, H., Ren, H., Yan, G., Wan, Z., Trigo, I. F., & Sobrino, J. A., 2013. Satellite-derived land surface temperature: Current status and perspectives. *Remote Sensing of Environment*. 131, 14-37. https://doi.org/10.1016/j.rse.2012.12.008

Li, Z., & Hu, D., 2022. Exploring the relationship between the 2D/3D architectural morphology and urban land surface temperature based on a boosted regression tree: A case study of Beijing, China. *Sustainable Cities and Society*. 78, 103392. https://doi.org/10.1016/j.scs.2021.103392

Liu, H., & Weng, Q., 2009. Scaling effect on the relationship between landscape pattern and land surface temperature.

Photogrammetric Engineering & Remote Sensing. 75(3), 291-304. https://doi.org/10.14358/PERS.75.3.291

Liu, X., Zhou, Y., Yue, W., Li, X., Liu, Y., & Lu, D., 2020. Spatiotemporal patterns of summer urban heat island in Beijing, China using an improved land surface temperature. *Journal of Cleaner Production*. 257, 120529. https://doi.org/10.1016/j.jclepro.2020.120529

Liu, Y., Wang, Z., Liu, X., & Zhang, B., 2021. Complexity of the relationship between 2D/3D urban morphology and the land surface temperature: a multiscale perspective. *Environmental Science and Pollution Research*. 28(47), 66804-66818. https://doi.org/10.1007/s11356-021-15177-7

Liu, Z., He, C., Zhang, Q., Huang, Q., & Yang, Y., 2012. Extracting the dynamics of urban expansion in China using DMSP-OLS nighttime light data from 1992 to 2008. *Landscape and Urban Planning*. 106(1), 62-72. https://doi.org/10.1016/j.landurbplan.2012.02.013

Lu, Y., Yue, W., Liu, Y., & Huang, Y., 2021. Investigating the spatiotemporal non-stationary relationships between urban spatial form and land surface temperature: A case study of Wuhan, China. *Sustainable Cities and Society*. 72, 103070. https://doi.org/10.1016/j.scs.2021.103070

Luo, X., Yang, J., Sun, W., & He, B., 2021. Suitability of human settlements in mountainous areas from the perspective of ventilation: A case study of the main urban area of Chongqing. *Journal of Cleaner Production*. 310, 127467. https://doi.org/10.1016/j.jclepro.2021.127467

Maimaitiyiming, M., Ghulam, A., Tiyip, T., Pla, F., Latorre-Carmona, P., Halik, Ü., Sawut, M., & Caetano, M., 2014. Effects of green space spatial pattern on land surface temperature: Implications for sustainable urban planning and climate change adaptation. *ISPRS Journal of Photogrammetry and Remote Sensing*. 89, 59-66. https://doi.org/10.1016/j.isprsjprs.2013.12.010

Moritz, C., & Agudo, R., 2013. The future of species under climate change: Resilience or decline? *Science*. 341(6145), 504-508. https://doi.org/10.1126/science.1237190

Müller, D., Leitão, P. J., & Sikor, T., 2013. Comparing the determinants of cropland abandonment in Albania and Romania using boosted regression trees. *Agricultural Systems*. 117, 66-77. https://doi.org/10.1016/j.agsy.2012.12.010

Oke, T. R., 1973. City size and the urban heat island. *Atmospheric Environment (1967)*. 7(8), 769-779. https://doi.org/10.1016/0004-6981(73)90140-6

Park, Y., Guldmann, J., & Liu, D., 2021. Impacts of tree and building shades on the urban heat island: Combining remote sensing, 3D digital city and spatial regression approaches. *Computers, Environment and Urban Systems*. 88, 101655. https://doi.org/10.1016/j.compenvurbsys.2021.101655

Patz, J. A., Campbell-Lendrum, D., Holloway, T., & Foley, J. A., 2005. Impact of regional climate change on human health. *Nature*. 438(7066), 310-317. https://doi.org/10.1038/nature04188

Peng, J., Jia, J., Liu, Y., Li, H., & Wu, J., 2018. Seasonal contrast of the dominant factors for spatial distribution of land surface temperature in urban areas. *Remote Sensing of Environment*. 215, 255-267. https://doi.org/10.1016/j.rse.2018.06.010

Peng, J., Liu, Q., Xu, Z., Lyu, D., Du, Y., Qiao, R., & Wu, J., 2020. How to effectively mitigate urban heat island effect? A perspective of waterbody patch size threshold. *Landscape and Urban Planning*. 202, 103873. https://doi.org/10.1016/j.landurbplan.2020.103873

Peng, S., Piao, S., Ciais, P., Friedlingstein, P., Ottle, C., Bréon, F., Nan, H., Zhou, L., & Myneni, R. B., 2012. Surface Urban Heat Island Across 419 Global Big Cities. *Environmental Science & Technology*. 46(2), 696-703. https://doi.org/10.1021/es2030438

Qiao, Z., Tian, G., & Xiao, L., 2013. Diurnal and seasonal impacts of urbanization on the urban thermal environment:

A case study of Beijing using MODIS data. *ISPRS Journal of Photogrammetry and Remote Sensing*. 85, 93-101. https://doi.org/10.1016/j.isprsjprs.2013.08.010

Qin, Z., Karnieli, A., & Berliner, P., 2001. A mono-window algorithm for retrieving land surface temperature from Landsat TM data and its application to the Israel-Egypt border region. *International Journal of Remote Sensing*. 22(18), 3719-3746. https://doi.org/10.1080/01431160010006971

Seto, K. C., Fragkias, M., Güneralp, B., & Reilly, M. K., 2011. A Meta-Analysis of Global Urban Land Expansion. *PLOS ONE*. 6(8), e23777. https://doi.org/10.1371/journal.pone.0023777

Stewart, I. D., Oke, T. R., & Krayenhoff, E. S., 2014. Evaluation of the 'local climate zone' scheme using temperature observations and model simulations. *International Journal of Climatology*. 34(4), 1062-1080. https://doi.org/10.1002/joc.3746

Sun, F., Mejia, A., & Che, Y., 2019. Disentangling the Contributions of Climate and Basin Characteristics to Water Yield Across Spatial and Temporal Scales in the Yangtze River Basin: A Combined Hydrological Model and Boosted Regression Approach. *Water Resources Management*. 33(10), 3449-3468. https://doi.org/10.1007/s11269-019-02310-y

Tong, L., Hu, S., & Frazier, A. E., 2018. Mixed accuracy of nighttime lights (NTL)-based urban land identification using thresholds: Evidence from a hierarchical analysis in Wuhan Metropolis, China. *Applied Geography*. 98, 201-214. https://doi.org/10.1016/j.apgeog.2018.07.017

Wan, Z., 2008. New refinements and validation of the MODIS Land-Surface Temperature/Emissivity products. *Remote Sensing of Environment*. 112(1), 59-74. https://doi.org/10.1016/j.rse.2006.06.026

Wang, Y., Sheng, S., & Xiao, H., 2021. The cooling effect of hybrid land-use patterns and their marginal effects at the neighborhood scale. *Urban Forestry & Urban Greening*. 59, 127015. https://doi.org/10.1016/j.ufug.2021.127015

Weng, Q., 2009. Thermal infrared remote sensing for urban climate and environmental studies: Methods, applications, and trends. *ISPRS Journal of Photogrammetry and Remote Sensing*. 64(4), 335-344. https://doi.org/10.1016/j.isprsjprs.2009.03.007

Wu, C., Li, J., Wang, C., Song, C., Chen, Y., Finka, M., & La Rosa, D., 2019. Understanding the relationship between urban blue infrastructure and land surface temperature. *Science of The Total Environment*. 694, 133742. https://doi.org/10.1016/j.scitotenv.2019.133742

Yang, C., Zhu, W., Sun, J., Xu, X., Wang, R., Lu, Y., Zhang, S., & Zhou, W., 2021b. Assessing the effects of 2D/3D urban morphology on the 3D urban thermal environment by using multi-source remote sensing data and UAV measurements: A case study of the snow-climate city of Changchun, China. *Journal of Cleaner Production*. 321, 128956. https://doi.org/10.1016/j.jclepro.2021.128956

Yang, J., Jin, S., Xiao, X., Jin, C., Xia, J. C., Li, X., & Wang, S., 2019. Local climate zone ventilation and urban land surface temperatures: Towards a performance-based and wind-sensitive planning proposal in megacities. *Sustainable Cities and Society*. 47, 101487. https://doi.org/10.1016/j.scs.2019.101487

Yang, J., Su, J., Xia, J., Jin, C., Li, X., & Ge, Q., 2018. The impact of spatial form of urban architecture on the urban thermal environment: A case study of the Zhongshan District, Dalian, China. *IEEE Journal of Selected Topics in Applied Earth Observations and Remote Sensing*. 11(8), 2709-2716. https://doi.org/10.1109/JSTARS.2018.2808469

Yang, J., Yang, Y., Sun, D., Jin, C., & Xiao, X., 2021a. Influence of urban morphological characteristics on thermal environment. *Sustainable Cities and Society*. 72, 103045. https://doi.org/10.1016/j.scs.2021.103045

Yang, J., Zhan, Y., Xiao, X., Xia, J. C., Sun, W., & Li, X., 2020. Investigating the diversity of land surface temperature

characteristics in different scale cities based on local climate zones. *Urban Climate*. 34, 100700. https://doi.org/10.1016/j.uclim.2020.100700

Yao, R., Wang, L., Huang, X., Gong, W., & Xia, X., 2019. Greening in Rural Areas Increases the Surface Urban Heat Island Intensity. *Geophysical Research Letters*. 46(4), 2204-2212. https://doi.org/10.1029/2018GL081816

Yao, R., Wang, L., Huang, X., Niu, Z., Liu, F., & Wang, Q., 2017. Temporal trends of surface urban heat islands and associated determinants in major Chinese cities. *Science of The Total Environment*. 609, 742-754. https://doi.org/10.1016/j.scitotenv.2017.07.217

Yao, R., Wang, L., Huang, X., Sun, L., Chen, R., Wu, X., Zhang, W., & Niu, Z., 2021. A Robust Method for Filling the Gaps in MODIS and VIIRS Land Surface Temperature Data. *IEEE Transactions on Geoscience and Remote Sensing*. 59(12), 10738-10752. https://doi.org/10.1109/TGRS.2021.3053284

Yu, B., Tang, M., Wu, Q., Yang, C., Deng, S., Shi, K., Chen, P., Wu, J., & Chen, Z., 2018. Urban built-up area extraction from log- transformed NPP-VIIRS nighttime light composite data. *IEEE Geoscience and Remote Sensing Letters*. 15(8), 1279-1283. https://doi.org/10.1109/LGRS.2018.2830797

Yu, S., Chen, Z., Yu, B., Wang, L., Wu, B., Wu, J., & Zhao, F., 2020b. Exploring the relationship between 2D/3D landscape pattern and land surface temperature based on explainable eXtreme Gradient Boosting tree: A case study of Shanghai, China. *Science of The Total Environment*. 725, 138229. https://doi.org/10.1016/j.scitotenv.2020.138229

Yu, Z., Yang, G., Zuo, S., Jørgensen, G., Koga, M., & Vejre, H., 2020a. Critical review on the cooling effect of urban blue-green space: A threshold-size perspective. *Urban Forestry & Urban Greening*. 49, 126630. https://doi.org/10.1016/j.ufug.2020.126630

Yuan, B., Zhou, L., Dang, X., Sun, D., Hu, F., & Mu, H., 2021a. Separate and combined effects of 3D building features and urban green space on land surface temperature. *Journal of Environmental Management*. 295, 113116. https://doi.org/10.1016/j.jenvman.2021.113116

Yuan, B., Zhou, L., Dang, X., Sun, D., Hu, F., & Mu, H., 2021b. Separate and combined effects of 3D building features and urban green space on land surface temperature. *Journal of Environmental Management*. 295, 113116. https://doi.org/10.1016/j.jenvman.2021.113116

Yue, W., Liu, X., Zhou, Y., & Liu, Y., 2019b. Impacts of urban configuration on urban heat island: An empirical study in China mega-cities. *Science of The Total Environment*. 671, 1036-1046. https://doi.org/10.1016/j.scitotenv.2019.03.421

Yue, W., Qiu, S., Xu, H., Xu, L., & Zhang, L., 2019a. Polycentric urban development and urban thermal environment: A case of Hangzhou, China. *Landscape and Urban Planning*. 189, 58-70. https://doi.org/10.1016/j.landurbplan.2019.04.008

Zeng, P., Sun, F., Liu, Y., Tian, T., Wu, J., Dong, Q., Peng, S., & Che, Y., 2022. The influence of the landscape pattern on the urban land surface temperature varies with the ratio of land components: Insights from 2D/3D building/vegetation metrics. *Sustainable Cities and Society*. 78, 103599. https://doi.org/10.1016/j.scs.2021.103599

Zhang, Y., Middel, A., & Turner, B. L., 2019. Evaluating the effect of 3D urban form on neighborhood land surface temperature using Google Street View and geographically weighted regression. *Landscape Ecology*. 34(3), 681-697. https://doi.org/10.1007/s10980-019-00794-y

Zhou, D., Xiao, J., Bonafoni, S., Berger, C., Deilami, K., Zhou, Y., Frolking, S., Yao, R., Qiao, Z., & Sobrino, J. A., 2019. Satellite Remote Sensing of Surface Urban Heat Islands: Progress, Challenges, and Perspectives. *Remote Sensing*. 11(1). https://doi.org/10.3390/rs11010048

Zhou, Y., Li, X., Asrar, G. R., Smith, S. J., & Imhoff, M., 2018. A global record of annual urban dynamics (1992–2013) from nighttime lights. *Remote Sensing of Environment*. 219, 206-220. https://doi.org/10.1016/j.rse.2018.10.015